Available online at www.sciencedirect.com
SCIENCE DIRECT®
Coordination Chemistry Reviews 249 (2005) 1296–1309
COORDINATION CHEMISTRY REVIEWS
www.elsevier.com/locate/ccr

Review

Structural and spectroscopic evidence for weak metal–metal interactions and metal–substrate exciplex formations in d^{10} metal complexes

Chi-Ming Che *, Siu-Wai Lai

Department of Chemistry and HKU-CAS Joint Laboratory on New Materials, The University of Hong Kong, Pokfulam Road, Hong Kong

Received 5 August 2004; accepted 15 November 2004
Available online 25 February 2005

Contents

Abstract

Structural investigations of homometallic di- and tri-nuclear coinage metal complexes with bridging phosphine ligands, $[M_2(P^{\cap}P)_2]X_2$ and $[M_3(P^{\cap}P^{\cap}P)_2]X_3$ (M = Cu(I), Au(I), and Ag(I); X = anion), have revealed close intramolecular metal–metal and metal–anion contacts in their crystal lattices, thus providing solid-state evidence for metallophilicity and metal–substrate interactions in two-coordinate d^{10} metal ions. To verify the existence of weak closed-shell metal–metal interactions, UV–vis absorption and resonance Raman spectroscopic techniques have been employed. Comparisons of the absorption spectra of $[M_2(P^{\cap}P)_2]^{2+}$ and $[M_3(P^{\cap}P^{\cap}P)_2]^{3+}$ show that the spin- and dipole-allowed $[nd\sigma^* \rightarrow (n+1)p\sigma]$ transition red-shifts in energy from $[M_2(P^{\cap}P)_2]^{2+}$ to $[M_3(P^{\cap}P^{\cap}P)_2]^{3+}$. This spectral assignment was confirmed by resonance Raman spectroscopy, which reveals stronger metal–metal interaction in the $^1[(n+1)p\sigma, nd\sigma^*]$ state compared to the ground state. Photoluminescence from the $^3[(n+1)p\sigma, nd\sigma^*]$ excited state was also recorded for the $[M_2(P^{\cap}P)_2]X_2$ and $[M_3(P^{\cap}P^{\cap}P)_2]X_3$ solids, where X is a non-coordinating anion. The spectroscopic data for these metal-centered transitions are supported by theoretical calculations. Perturbations of the M–M bonded excited states through interaction with neighboring solvent molecules or anions lead to exciplex formations with emission in the visible region. The sensitivity of photoluminescence of two-coordinate d^{10} metal complexes to metal-ligand coordination provides an entry to new classes of luminescent sensory materials for substrate-binding processes. The $^3[(n+1)p\sigma, nd\sigma^*]$ excited states of $[M_2(P^{\cap}P)_2]^{2+}$ (M = Cu and Au) systems are powerful reductants and light-induced multi-electron photocatalysis by these systems have been observed.
© 2005 Elsevier B.V. All rights reserved.

Keywords: Closed shell; Metallophilicity; Exciplex; Luminescence; Spectroscopy

1. Introduction

The most widely studied excited-state chemistry that involves weak metal–metal interaction in the ground state and enhanced metal–metal interaction in the excited state is $[Pt_2(\mu\text{-}P_2O_5H_2)_4]^{4-}$ [1]. Square-planar Pt(II) with vacant axial coordination site facilitates substrate binding reactions and the photochemistry mediated by $[Pt_2(\mu\text{-}P_2O_5H_2)_4]^{4-}$ includes atom abstraction, electron transfer, and inorganic exciplex formation [1b]. However, the reactivity of $[Pt_2(\mu\text{-}P_2O_5H_2)_4]^{4-}$ remains unique because structural modification

* Corresponding author. Tel.: +852 2859 2154; fax: +852 2857 1586.
E-mail address: cmche@hku.hk (C.-M. Che).

0010-8545/$ – see front matter © 2005 Elsevier B.V. All rights reserved.
doi:10.1016/j.ccr.2004.11.026

is difficult. Thus, there is an impetus to develop new classes of coordinatively unsaturated metal photocatalysts for light-induced atom transfer and excited-state substrate-binding reactions. In this context, photoluminescent d^{10} metal complexes with low coordination numbers have become a target for our studies over the past several years. Closed-shell d^{10} metal complexes are known to exhibit photoluminescent properties that are perturbed through subtle changes in the environment, which the complexes are located.

Dori and co-workers first reported the intriguing photoluminescence of d^{10} metal complexes [2]. In the paper published in 1986, Vogler and Kunkely reported the photoluminescence of tetrameric copper(I) iodide complexes in solution. The remarkable finding is that while the $[Cu(L)I]_4$ complexes (L = pyridine, morpholine) do not display any significant absorption at $\lambda > 350$ nm, they emit strongly at $\lambda_{max} = 650$–700 nm in solution [3]. Such a large Stoke's shift between the absorption and emission energies suggests a strongly distorted excited state whose structure is significantly different from the ground state. In 1989, Fackler and co-workers [4] and Che et al. [5] independently reported the spectroscopic properties and excited-state redox chemistry of $[Au_2(dppm)_2]^{2+}$ (dppm = bis(diphenylphosphino)methane). This complex displays strong and long-lived phosphorescence at $\lambda_{max} = 593$ nm ($\tau = 21$ μs and $\phi = 0.31$) in solution [4] that was attributed to Au–Au bonded excited state. The $[Au_2(dppm)_2]^{2+*}$ excited state is a powerful reductant, with an E° value of $-1.6(1)$ V versus SSCE (saturated sodium chloride calomel electrode) according to Che's work [6], and catalyzes light-induced C–X bond cleavage from benzyl halides [7]. These reports on the photophysical properties of $[Au_2(dppm)_2]^{2+}$ have subsequently generated interest from different research groups to develop photoluminescent gold(I) complexes [8].

It is well recognized that metallophilic interactions between closed-shell d^{10} metal ions can result in aggregation to dimers, oligomers, chains and sheets [9–11], and most of these compounds are strongly emissive. In the literature, various spectroscopic assignments have been put forward to account for the photoluminescent properties of polynuclear d^{10} metal complexes. A metal–metal bonded excited state is typically invoked [8], and recently ligand-to-metal charge-transfer excited states have also been proposed for the photoluminescence of polynuclear d^{10} chalcogenide complexes [12]. However, spectroscopic characterization for the metal–metal bonded excited states, usually denoted $[(n+1)p\sigma, nd\sigma^*]$ or for ligand-to-metal charge-transfer excited states of d^{10} metal complexes remains sparse.

It is a general phenomenon that the photoluminescent properties of polynuclear d^{10} metal complexes are sensitively affected by subtle structural and/or environmental changes. For example, variations of emission properties in polynuclear d^{10} metal complexes upon exposure to volatile organic compounds had been observed by Balch, Eisenberg, and Ford [13]. Catalano et al. reported a tetranuclear silver(I) cluster, which undergoes significant changes in emission properties in the presence of CO [14]. Such findings would indicate that other factors apart from metal–metal interactions are affecting the photoluminescence of polynuclear d^{10} metal complexes. In 1992, McCleskey and Gray reported an intensely emissive three-coordinate $[Au_2(dcpe)_3](PF_6)_2$ (dcpe = 1,2-bis(dicyclohexylphosphino)ethane) complex [15], thus highlighting the importance of gold-ligand coordination upon the photoluminescent properties of Au(I) complexes. Subsequently, we reported that the visible emission of the $[M_2(dcpm)_2]X_2$ (dcpm = bis(dicyclohexylphosphino)methane) systems originate from metal–anion/solvent exciplex formation [16].

2. Structural evidence for metal–metal and metal–anion/solvent interactions

The M(I)–M(I) distances provide an indicator for metallophilicity. M–M contacts that are shorter than the sum of the van der Waals radii (2.80 Å for Cu–Cu, 3.32 Å for Au–Au, and 3.44 Å for Ag–Ag [17]) are possibly prone to attractive homodinuclear interactions. In the $[M_2(P^{\cap}P)_2]X_2$ systems described in the following section, the M–M distances are dependent upon the nature of the counter-anion, and this can be attributed to the interaction between the $[M_2(P^{\cap}P)_2]^{2+}$ core and X^-.

The intramolecular Cu···Cu separations in $[Cu_2(dcpm)_2](ClO_4)_2$ and $[Cu_2(dcpm)_2](PF_6)_2$ are 2.685 (av.) and 2.790(5) Å, respectively, while those in $[Cu_2(dcpm)_2(CH_3CN)_2]X_2$ ($X = ClO_4^-$ and PF_6^-) are 2.8096(9) and 2.810(2) Å, respectively [16b]. The average Cu···Cu distance of $[Cu_2(dcpm)_2]I_2$ is 2.905 Å (Fig. 1), which is the longest among the $[Cu_2(dcpm)_2]X_2$ complexes studied in this work. Such a long Cu–Cu distance can be attributed to the coordination of I^- to Cu(I), which weakens the intramolecular metal–metal interaction. Indeed, the counter-anions in $[Cu_2(dcpm)_2]X_2$ ($X = ClO_4^-$ and PF_6^-) have been found to interact weakly with Cu(I) in trigonal fashion, with the nearest Cu···O and Cu···F distances being 2.558(6) and 2.79(1) Å, respectively (Fig. 2). The structures of $[Cu_2(dcpm)_2(CH_3CN)_2]X_2$ ($X = ClO_4^-$ and PF_6^-) reveal coordination of CH_3CN to each Cu(I) core, affording a Y-shaped trigonal P_2CuN configuration (Fig. 3).

Replacement of the dcpm ligand with dppm leads to an increase in the Cu–Cu separation. A long Cu···Cu distance of 3.757(3) Å was observed in $[Cu_2(dppm)_2(CH_3CN)_4](ClO_4)_2$ [18], in which the Cu atoms adopt a pseudo-tetrahedral geometry. Similarly, previous reports on $[Cu_2(\mu\text{-dppm})_2(py)_2]^{2+}$ (py = substituted pyridines) complexes also revealed long Cu···Cu separations (>3.7 Å) [19]. It should be noted that even with a sterically bulky phosphine ligand, Cu(I)–anion interactions have also been observed in the mononuclear $[Cu(PCy_3)_2]ClO_4$ compound, in which a trigonal $P_2Cu(O–ClO_3)$ configuration was observed.

We reported the crystal structure of $[Cu_3(dpmp)_2(MeCN)_2(\mu\text{-Cl})_2]ClO_4$ (dpmp = bis(diphenylphosphinom-

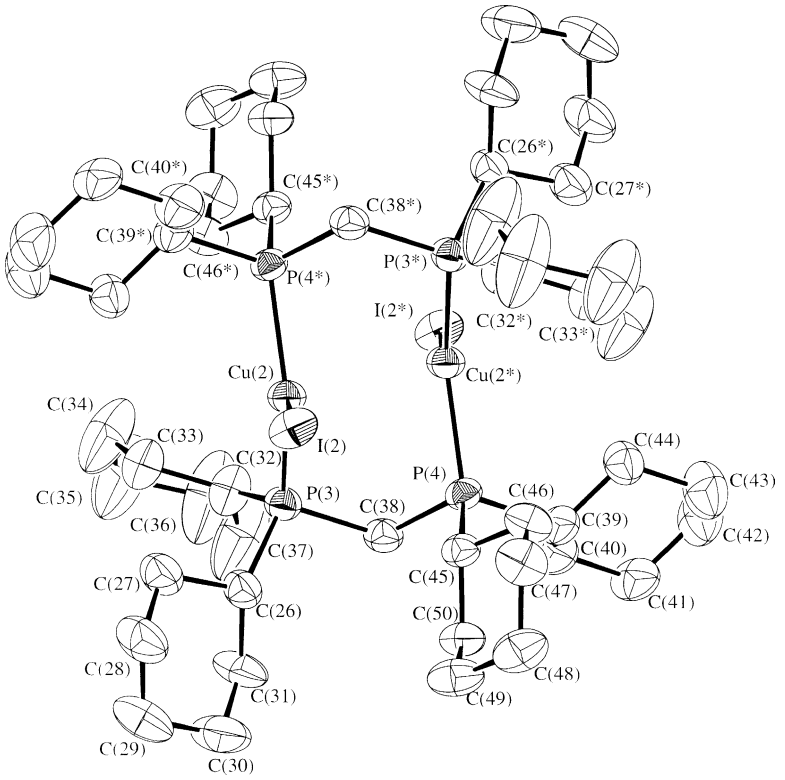

Fig. 1. Perspective view of $[Cu_2(\mu\text{-dcpm})_2]I_2$ (Reprinted with permission from Ref. [16d]. Copyright (2003) Wiley–VCH).

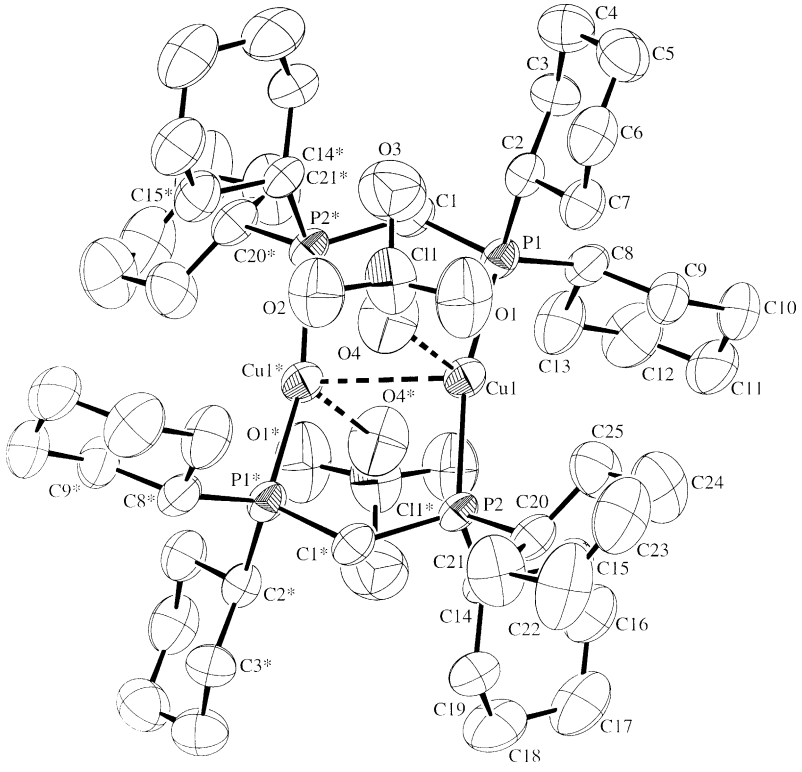

Fig. 2. Perspective view of $[Cu_2(\mu\text{-dcpm})_2](ClO_4)_2$ (Reprinted with permission from Ref. [16d]. Copyright (2003) Wiley–VCH).

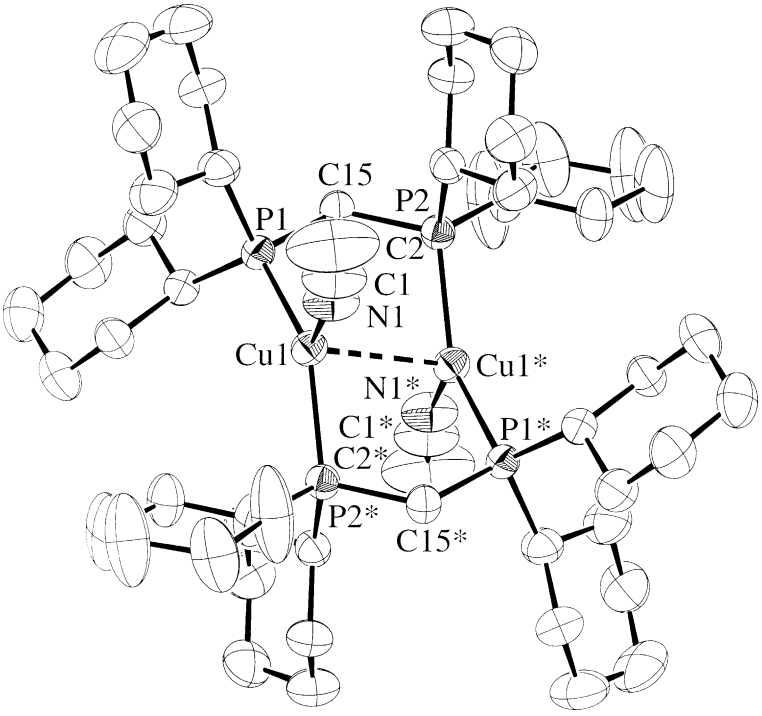

Fig. 3. Perspective view of the cation of $[Cu_2(\mu\text{-dcpm})_2(CH_3CN)_2](ClO_4)_2$ (Reprinted with permission from Ref. [16d]. Copyright (2003) Wiley–VCH).

ethyl)phenylphosphine) [20], which consists of three Cu(I) ions in distorted tetrahedral geometry bridged by two dpmp ligands and two chloride ions, plus two acetonitrile molecules at the two terminal Cu(I) sites (Fig. 4). The intramolecular Cu···Cu separations are 3.26 and 3.30 Å, thus indicating no Cu(I)–Cu(I) interaction. The average P–Cu–P angle is 118.7°, which deviates markedly from linearity.

For $[Ag_2(\mu\text{-dcpm})_2]X_2$ and its derivatives, we have also observed close Ag(I)-anion contacts [21]. Complex $[(Cy_3P)Ag(O_2CCF_3)]_2$ crystallizes in a dimeric form, with two $[(Cy_3P)Ag(O_2CCF_3)]$ units (P–Ag–O = 160.7(2)°) held together by a Ag–Ag separation of 3.095(1) Å (Fig. 5). The crystal structure of $[Ag_2(\mu\text{-dcpm})(\mu\text{-}O_2CCF_3)_2]$ reveals short and long Ag–O(acetate) separations (2.191(3) and 2.446(4) Å, respectively), plus a silver–silver distance of 2.8892(9) Å (Fig. 6). The molecular structures of $[Ag_2(\mu\text{-dcpm})_2](CF_3SO_3)_2$ and $[Ag_2(\mu\text{-dcpm})_2](PF_6)_2$ (Fig. 7) contain $Ag_2P_4C_2$ cores that adopt chair conformations. The average silver–silver separation is 2.948 Å in the former and 2.923 Å in the latter, which are typical for polynuclear Ag(I) derivatives with proposed Ag(I)–Ag(I) interactions [22]. A slightly longer Ag–Ag distance of 3.041(2) Å was reported for the analogous complex $[Ag_2(\mu\text{-dmpm})_2](PF_6)_2$ [23] (dmpm = bis(dimethylphosphino)methane). Ho and Bau [22a] reported the structure of $[Ag_2(dppm)_2(NO_3)_2]$ with an intramolecular Ag–Ag separation of 3.085(1) Å, which is longer than the related values of 2.907–2.960 Å in $[Ag_2(\mu\text{-dcpm})_2]X_2$ ($X = CF_3SO_3^-$ and PF_6^-) [21].

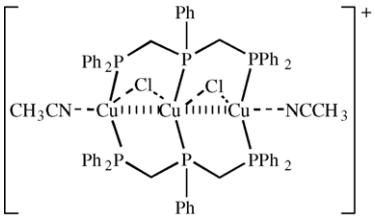

Fig. 4. Structure of $[Cu_3(\mu\text{-dpmp})_2(MeCN)_2(\mu\text{-Cl})_2]^+$ [20].

Close Ag-anion contacts are evident in the crystal lattices of $[Ag_2(\mu\text{-dcpm})_2](CF_3SO_3)_2$ (Ag···O 2.692(7) Å) [21] and $[Ag_2(\mu\text{-dcpm})_2](PF_6)_2$ (Ag···F 2.64(5) Å) [21] where one anion is associated with one Ag(I) site resulting in a Ag–Ag–O/F angle of ∼90°, and the other similarly interacts with Ag(I) at the opposite side of the Ag_2P_4 plane. It should be noted that such interactions are not apparent in the crystal structure of the gold(I) congener, $[Au_2(\mu\text{-dcpm})_2](ClO_4)_2$ [16a].

We have reported the structure of $[Ag_3(dpmp)_2(CH_3CN)_2(ClO_4)_2]ClO_4\cdot(Et_2O)_2$ (dpmp = bis(diphenylphosphinomethyl)phenylphosphine [24], which consists of three Ag(I) centres bridged by a pair of dpmp ligands arranged in a *trans* configuration, plus two perchlorate ions and two acetonitrile molecules weakly coordinated to the silver atoms (Fig. 8). The intramolecular Ag···Ag distances are 2.943(2) and 3.014(2) Å, which are slightly shorter than those of 3.085 Å in $[Ag_2(dppm)_2(NO_3)_2]$ [22a] and 3.192(3)–3.362(3) Å in $[Ag_3(dppm)_3Br_2]Br$ [25]. One Ag(I) ion interacts with both the ClO_4^- ion and CH_3CN molecule, leading to severely bending of the corresponding P–Ag–P

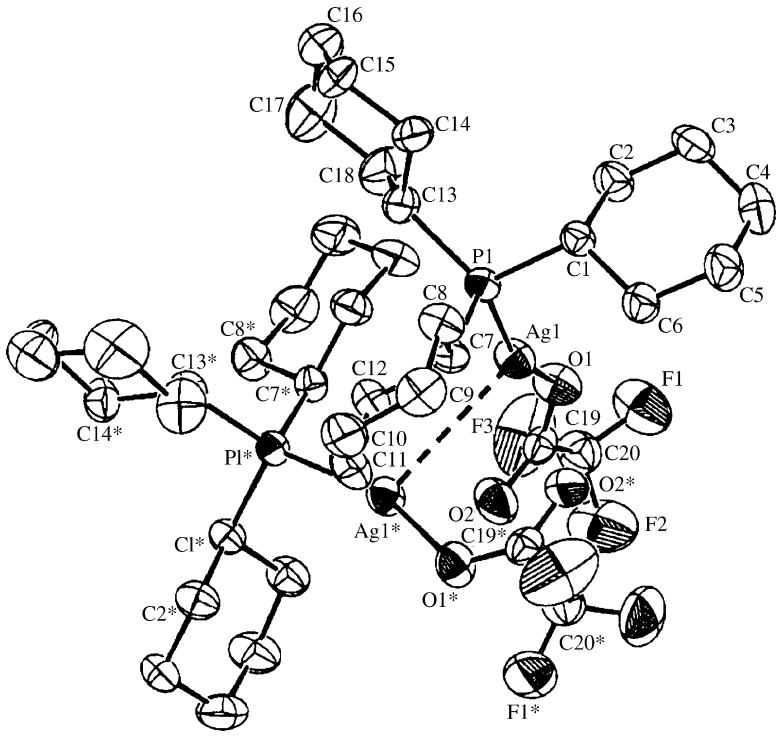

Fig. 5. Perspective view of $[(Cy_3P)Ag(O_2CCF_3)]_2$ (Reprinted with permission from Ref. [21]. Copyright (2000) American Chemical Society).

angle to 137.9(1)°. The Ag–Ag–Ag angle of 175.33(7)° is close to linearity.

The crystal structures of $[Au_2(dppm)_2]X_2$ have been extensively studied [4–6,26–28] prior to our investigations on the $[Au_2(dcpm)_2]X_2$ solids [16a,c]. The crystal structure of $[Au_2(dppm)_2](BH_3CN)_2$ shows a Au···Au separation of 2.982(2) Å with a short cation–anion Au···H(BH_2CN) contact (2.96(8) Å) [29]. For the complex cation in

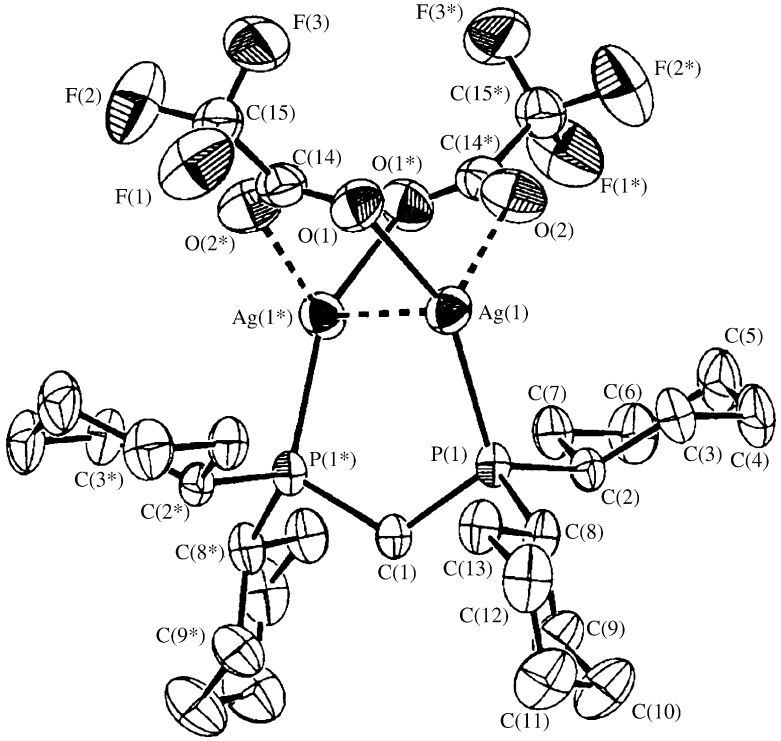

Fig. 6. Perspective view of $[Ag_2(\mu\text{-dcpm})(\mu\text{-}O_2CCF_3)_2]$ (Reprinted with permission from Ref. [21]. Copyright (2000) American Chemical Society).

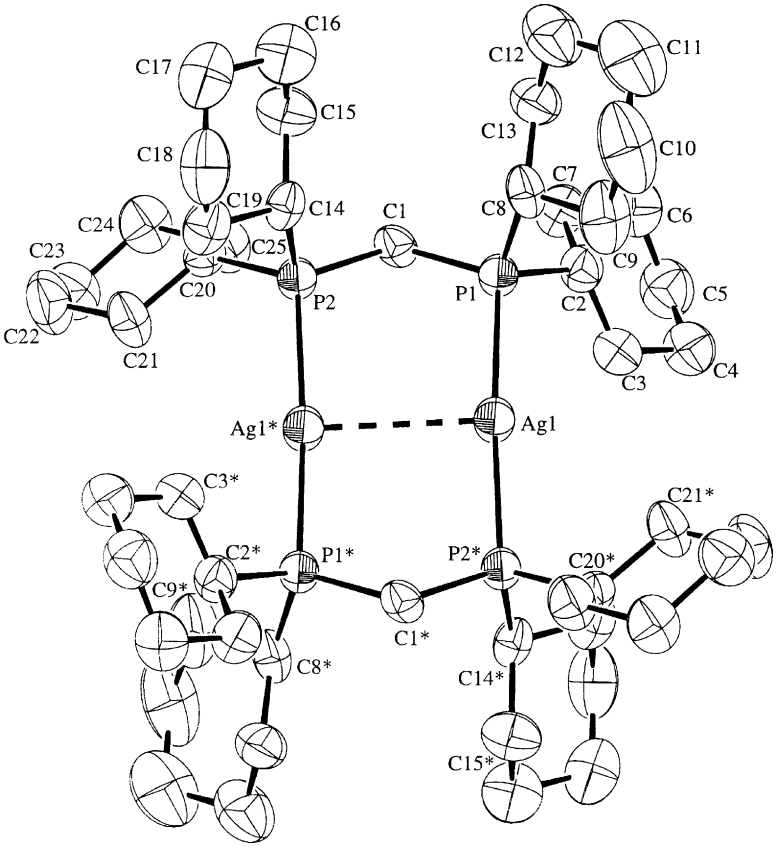

Fig. 7. Perspective view of cation in $[Ag_2(\mu\text{-dcpm})_2](PF_6)_2$ (Reprinted with permission from Ref. [21]. Copyright (2000) American Chemical Society).

$[Au_2(dppm)_2I][Au(CN)_2]$, the two Au(I) are bridged by iodide with Au–I distances of 3.161(3) and 3.342(3) Å and Au–Au–I angle of 73°. The intramolecular Au···Au separation is 2.967(1) Å, while the P–Au–P angles are only slightly perturbed from linearity (170 and 171°). The crystal structure of the cation in $[Au_2(dppm)_2(S_2CNEt_2)](BH_3CN)$ shows that $S_2CNEt_2^-$ bridges two gold atoms by forming Au–S bonds (2.648(3) and 2.703(3) Å). Greater deviations of the P–Au–P angles in $[Au_2(dppm)_2(S_2CNEt_2)]^+$ from linearity (160 and 154°) suggest that the Au–S interactions are stronger compared to Au–I in $[Au_2(dppm)_2(I)]^+$. The Au···Au distance in $[Au_2(dppm)_2(S_2CNEt_2)]^+$ is 2.949(1) Å, which is typical for $[Au_2(dppm)_2]X_2$ (X = Cl^- [26], NO_3^- [27], and BF_4^- [28]) compounds.

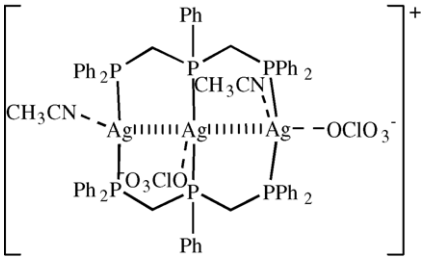

Fig. 8. Structure of $[Ag_3(\mu\text{-dpmp})_2(CH_3CN)_2(ClO_4)_2]^+$ [24].

The intramolecular Au–Au distances for $[Au_2(dcpm)_2]X_2$ are 2.9389(9), 2.9876(5), 2.9925(2), 2.9821(7), and 3.0756(6) Å for X = ClO_4^-, $Au(CN)_2^-$, Cl^-, SCN^-, and I^-, respectively [16c]. The structure of $[Au_2(dcpm)_2]I_2$ features a close Au···I contact of 2.9960(7) Å, which results in a T-shaped AuP_2I geometry (Fig. 9). Similarly, Au(I)–anion interactions, namely Au···$OClO_3^-$ (3.36(2) Å), Au···$Au(CN)_2^-$ (3.33(1) Å), Au···SCN^- (3.011(3) Å), and Au···Cl^- (2.7755(9) Å) have also been detected, although these distances are significantly longer than the Au–I separations in $[Au_2(dcpm)_2]I_2$. As discussed in the next section, these Au(I)-anion contacts can affect the photoluminescence of the $[Au_2(dcpm)_2]X_2$ solids. Cation–anion interactions have also been reported for the halide (Cl^-, Br^-, and I^-) salts of $[Au_2(dmpm)_2]^{2+}$ and $[Au_2(dmpe)_2]^{2+}$ (dmpe = bis(dimethylphosphino)ethane) [30]. The cation in $[Au_2(dcpe)_2](PF_6)_2$ consists of two Au atoms joined by two dcpe ligands [31], and the intramolecular Au···Au distance of 2.936(1) Å is comparable to that of 2.9389(9) Å in $[Au_2(dcpm)_2](ClO_4)_2$ [16c]. The structure of $[Au_2(dcpe)_3][Au(CN)_2]_2$ [32] shows that each Au atom is bound to one chelating dcpe and one bridging dcpe, and each AuP_3 unit has a distorted trigonal planar geometry (Fig. 10). The bridging dcpe ligand in $[Au_2(dcpe)_3]^{2+}$ extends the Au···Au separation to 7.0501 Å, which results in no Au–Au interaction.

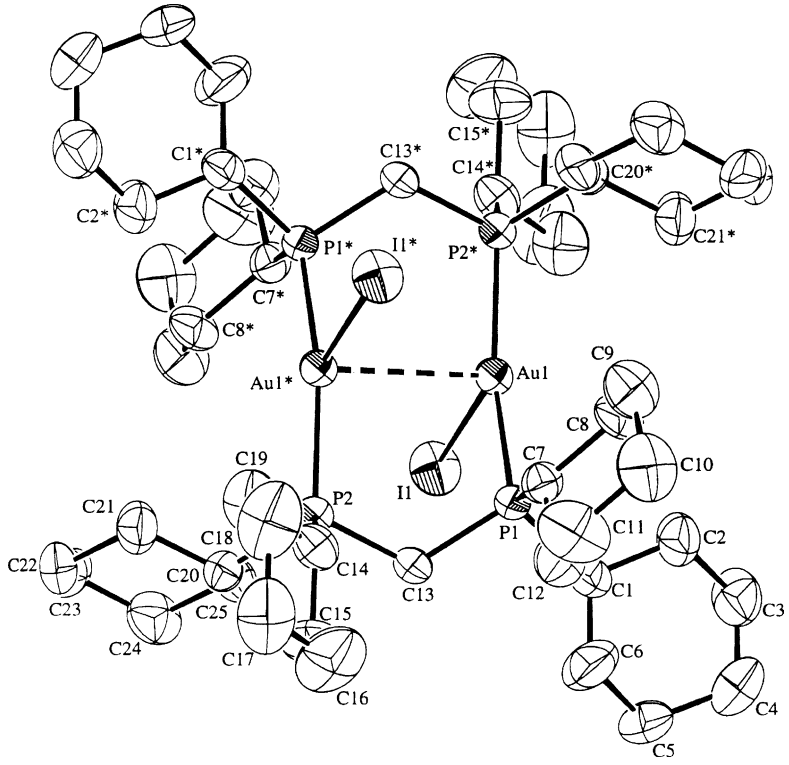

Fig. 9. Perspective view of $[Au_2(\mu\text{-dcpm})_2]I_2$ (Reprinted with permission from Ref. [16c]. Copyright (2001) Wiley–VCH).

We have previously reported the structures of $[Au_3(P^{\cap}P^{\cap}P)_2]X_3$ ($P^{\cap}P^{\cap}P$=dmmp=bis(dimethylphosphinomethyl)methylphosphine, X = ClO_4^- [33]; $P^{\cap}P^{\cap}P$ = dpmp = bis(diphenylphosphinomethyl)phenylphosphine, X = SCN^- [34]), which consist of three Au(I) ions held together by two bridging $P^{\cap}P^{\cap}P$ ligands, plus three non-coordinating anions (Fig. 11). In the $[Au_3(dmmp)_2]^{3+}$ cation [33], the Au–Au–Au angle of 136.26(4)° is greatly distorted from a linear geometry, and the intramolecular Au···Au distances of 2.981(1) and 2.962(1) Å are similar to those observed in binuclear Au(I) complexes [4–6,26–29]. The AuP_2 units are linear with P–Au–P angles ranging from 175.0(2)° to 176.2(2)°. The structure of the $[Au_3(dpmp)_2]^{3+}$ cation [34], on the other hand, shows that the Au_3 chain is nearly linear with the Au–Au–Au angle of 167.21(2)°,

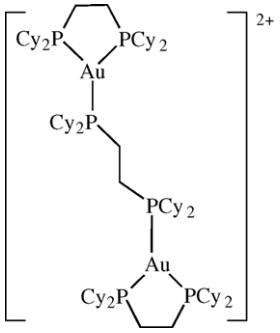

Fig. 10. Structure of $[Au_2(dcpe)_3]^{2+}$ [32].

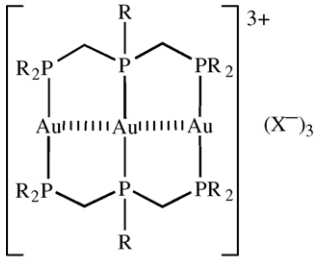

R = Me; X = ClO_4^- [33]

Ph; X = SCN^- [34]

Fig. 11. Structure of $[Au_3(P^{\cap}P^{\cap}P)_2]X_3$ [33,34].

and the intramolecular Au–Au distances are 3.0137(8) and 3.0049(8) Å. The three SCN^- ions are considered to be uncoordinated since the Au···SCN distances range from 2.947(4) to 3.717(7) Å.

3. Spectroscopic evidence for the ndσ* → (n + 1)pσ transitions

In general, the UV–vis absorption spectra of the $[M_2(dcpm)_2]^{2+}$ complexes reveal an intense spin- and dipole-allowed absorption band, which is absent from the mononuclear counterparts. Such a spectroscopic feature is attributed to a [ndσ* → (n + 1)pσ] transition described

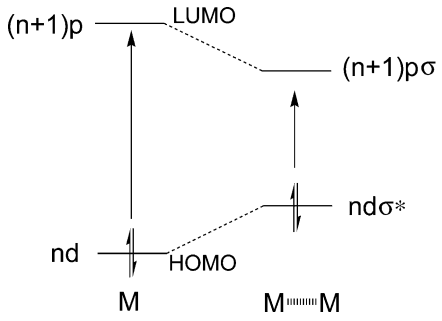

Scheme 1. Molecular orbital diagram illustrating d^{10}–d^{10} interaction in binuclear coinage metal complexes.

by the molecular orbital diagram depicted in Scheme 1. The [$nd\sigma^* \rightarrow (n+1)p\sigma$] transition features a large ε value (>10^4 dm^3 mol^{-1} cm^{-1}) and this assignment is supported by resonance Raman spectroscopic measurements, which reveal the M–M stretch fundamental and overtone bands [16b,21,35]. Specific details for the Au(I), Ag(I), and Cu(I) systems are now presented.

The electronic absorption spectrum of $[Au_2(dppm)_2](ClO_4)_2$ (dppm = bis(diphenylphosphino)methane) [4–6] in acetonitrile exhibits an intense absorption band at 290 nm attributable to the [$5d\sigma^* \rightarrow 6p\sigma$] transition, which is absent in $[Au\{P(OCH_2)_3CC_2H_5\}_2]^+$ [36] and $[Au\{P(C_2H_5)_3\}_2]^+$ [37]. We have employed sterically bulky and optically transparent phosphine ligands to examine the spectroscopic properties of Au(I)–phosphine complexes. The aliphatic PCy_3 and dcpm ligands are optically transparent in the UV region ($\lambda \geq 250$ nm), which allow the [$nd\sigma^* \rightarrow (n+1)p\sigma$] transition arisen from M(I)–M(I) interactions in the ground and excited states to be probed.

The $[Au_2(dcpm)_2]X_2$ (X = ClO_4^-, PF_6^-, $CF_3SO_3^-$, and $Au(CN)_2^-$) complexes exhibit an intense band at λ_{max} = 277 nm ($\varepsilon = 2.6 \times 10^4 - 2.9 \times 10^4$ dm^3 mol^{-1} cm^{-1}) and a weak shoulder at λ_{max} = 310 nm ($\varepsilon \approx 400$ dm^3 mol^{-1} cm^{-1}), which are assigned to the ^{1}[$5d\sigma^* \rightarrow 6p\sigma$] and ^{3}[$5d\sigma^* \rightarrow 6p\sigma$] transitions, respectively. McCleskey and Gray also reported similar spectral feature for the related $[Au_2(dcpe)_2]^{2+}$; this complex exhibits an intense band at 271 nm (ε = 10,000 dm^3 mol^{-1} cm^{-1}) and a weak absorption at 320 nm, which was assigned to the [$5d\sigma^*$, $6p\sigma$] singlet and triplet states, respectively [15].

Complex $[Au_2(dcpm)_2]I_2$ shows an intense absorption band at λ = 275 nm which has a similar band shape to the 277-nm absorption band of the $[Au_2(dcpm)_2]^{2+}$ ion, and hence can be assigned to $^1(5d\sigma^* \rightarrow 6p\sigma)$ transition. However, there are additional intense absorption bands with λ_{max} at 323 nm (ε = 6100 dm^3 mol^{-1} cm^{-1}) and 365 nm (sh, ε = 1300 dm^3 mol^{-1} cm^{-1}), while $[Au_2(dcpm)_2]X_2$ (X = ClO_4^-, PF_6^-, $CF_3SO_3^-$, $Au(CN)_2^-$, Cl^-, and SCN^-) absorb only weakly at $\lambda \geq 310$ nm. The two intense absorption bands of $[Au_2(dcpm)_2]I_2$ at 323 and 365 nm are attributed to ground-state Au–I interactions. The [$5d\sigma^* \rightarrow 6p\sigma$] transition has also been observed for the tri-nuclear gold(I) system. In acetonitrile, $[Au_3(dmmp)_2](ClO_4)_3$ exhibits an intense 315-nm absorption band (ε = 23,360 dm^3 mol^{-1} cm^{-1}) [33]. The red-shift in transition energy from the 271-nm absorption band of $[Au_2(dmpm)_2]^{2+}$ [30] is in accordance with the [$5d\sigma^* \rightarrow 6p\sigma$] assignment and signifies destabilization of the $d\sigma^*$ orbital upon increasing the number of AuP_2 units, which leads to narrowing of the $5d\sigma^*$–$6p\sigma$ gap.

Emission from the [$6p\sigma$, $5d\sigma^*$] excited state for the $[Au_2(P\cap P)_2]^{2+}$ system has been recorded. Upon excitation at 280 nm, $[Au_2(dcpm)_2]X_2$ (X = ClO_4^-, PF_6^-, $CF_3SO_3^-$, and $Au(CN)_2^-$) with non-coordinating anions exhibit intense phosphorescence with $\lambda_{max} \approx 368$ nm in the solid state at room temperature and in MeOH/EtOH (4:1) glassy solutions at 77 K. Time-resolved measurements revealed that the solid-state emission of $[Au_2(dcpm)_2](ClO_4)_2$ at 368 nm follows a single-exponential decay. The Stoke's shift from the 278-nm ^{1}[$5d\sigma^* \rightarrow 6p\sigma$] and 317-nm ^{3}[$5d\sigma^* \rightarrow 6p\sigma$] absorption bands to the room-temperature solid-state emission of $[Au_2(dcpm)_2](ClO_4)_2$ at 368 nm are 8800 and 4370 cm^{-1}, respectively. These are in good agreement with values from the analogous transitions in d^8–d^8 complexes [1b]. The ^{3}[$6p\sigma$, $5d\sigma^*$] emission of $[Au_2(dcpm)_2]X_2$ (X = ClO_4^-, PF_6^-, $CF_3SO_3^-$, and $Au(CN)_2^-$) has also been modelled by theoretical calculations. Using $[Au_2(H_2PCH_2PH_2)_2]^{2+}$ as a model, a high-energy emission at 331 nm was calculated from the ^3A_u excited state in the absence of anion or solvent exciplex formation [38]. The calculated emission energy matches the intense 368-nm solid-state emission of $[Au_2(dcpm)_2](ClO_4)_2$, which has an intramolecular Au···Au separation of 2.927 Å. Based on ab initio calculations, weak aurophilic attraction was found in the ground state of $[Au_2(H_2PCH_2PH_2)_2]^{2+}$, but the Au–Au interaction is greatly enhanced in the ^{3}[$6p\sigma$, $5d\sigma^*$] excited state. Such an increase in Au–Au bond strength in the excited state was similarly supported by resonance Raman spectroscopic measurements [35].

The low-temperature (77 K) solid-state emission of $[Au_2(dcpe)_2]^{2+}$ appears at λ_{max} = 489 nm. The emission spectrum of $[Au_3(dmmp)_2](ClO_4)_3$ in degassed acetonitrile shows dual phosphorescence at 467 and 580 nm [33]. The high-energy emission at 467 nm was previously attributed to spin-forbidden intraligand transition of the phosphine ligands, but it is appropriate to revise this assignment. We re-assign the 467-nm emission of $[Au_3(dmmp)_2](ClO_4)_3$ to originate from the ^{3}[$6p\sigma$, $5d\sigma^*$] excited state. The 580-nm emission is here assigned to come from binding of CH_3CN to the $[Au_3(dmmp)_2]^{3+}$ core in the excited state [39].

Spectroscopic evidence for metal–metal bonded [$5p\sigma$, $4d\sigma^*$] excited states in binuclear and polynuclear Ag(I) complexes remain sparse in the literature. Owing to the very weak Ag–Ag interaction and the considerable larger energy gap between the 4d and (5s, 5p) levels, the [$4d\sigma^* \rightarrow 5p\sigma$] transition can be easily obscured by intraligand [$\pi \rightarrow \pi^*$] transitions of arylphosphine ligands. In our studies, bulky, optically transparent phosphine ligands were employed and comparisons

were made between the absorption and emission properties of mono- and di-nuclear Ag(I) complexes. An intense absorption band is observed for $[Ag_2(\mu\text{-dcpm})_2]X_2$ ($X = CF_3SO_3^-$ and PF_6^-) at $\lambda_{max} = 266$ nm ($\varepsilon = 2.2 \times 10^4$ dm^3 mol^{-1} cm^{-1}) and for $[Ag_2(\mu\text{-dcpm})(\mu\text{-}O_2CCF_3)_2]$ at $\lambda_{max} = 243$ nm ($\varepsilon = 1.3 \times 10^4$ dm^3 mol^{-1} cm^{-1}) [21]. In contrast, the absorption spectra of $[Ag(PCy_3)(O_2CCF_3)]_2$ and $[Ag(PR_3)_2]ClO_4$ (R = Me and Cy) show ε values below 10^2 at $\lambda \geq 250$ nm. The high ε values and profiles of the prominent absorption bands of the $[Ag_2(\mu\text{-dcpm})_2]X_2$ system are characteristic of $[n\mathrm{d}\sigma^* \rightarrow (n+1)\mathrm{p}\sigma]$ transitions as observed for $[Au_2(P^{\frown}P)_2]^{2+}$ ($P^{\frown}P$ = dppm, dcpm) [4–6,16a,c,35]. Significantly, the $[4\mathrm{d}\sigma^* \rightarrow 5\mathrm{p}\sigma]$ absorption band for $[Ag_2(\mu\text{-dcpm})_2]X_2$ ($X = CF_3SO_3^-$ and PF_6^-) displays a slight blue-shift to 261 nm and broadening in acetonitrile solution ($\varepsilon = 1.7 \times 10^4$ dm^3 mol^{-1} cm^{-1}). We suggest that coordination of CH_3CN to Ag(I) would disrupt the intramolecular Ag–Ag interaction, which would consequently affect the $[4\mathrm{d}\sigma^* \rightarrow 5\mathrm{p}\sigma]$ transition. For the tri-nuclear complex $[Ag_3(dpmp)_2(CH_3CN)_2(ClO_4)_2]ClO_4\cdot(Et_2O)_2$, an absorption peak maximum at 288 nm ($\varepsilon = 2.53 \times 10^4$ dm^3 mol^{-1} cm^{-1}) was recorded in dichloromethane [24]. This absorption is blue-shifted from the 315-nm absorption band for the related $[Au_3(dmmp)_2]^{3+}$ complex in acetonitrile [33], and is assigned to the $^1[4\mathrm{d}\sigma^* \rightarrow 5\mathrm{p}\sigma]$ transition.

At 298 K, solid samples of $[Ag_2(\mu\text{-dcpm})_2]X_2$ ($X = CF_3SO_3^-$ and PF_6^-) exhibit photoluminescence at $\lambda_{max} = 417$–420 nm (lifetime ~0.5 μs). The large Stoke's shift of the solid emission maxima from the corresponding $[4\mathrm{d}\sigma^* \rightarrow 5\mathrm{p}\sigma]$ absorption band in acetonitrile (ca. 14,500 cm^{-1}) indicate that the solid-state emission of these Ag(I) solids do not solely originate from the $[5\mathrm{p}\sigma, 4\mathrm{d}\sigma^*]$ excited state [21]. The $[Ag_3(dpmp)_2(CH_3CN)_2(ClO_4)_2]ClO_4\cdot(Et_2O)_2$ solid emits at $\lambda_{max} =$ 467 nm at room temperature [24].

The $[3\mathrm{d}\sigma^* \rightarrow 4\mathrm{p}\sigma]$ transition in Cu(I) systems has not been reported prior to our work on the $[Cu_2(\mu\text{-dcpm})_2]X_2$ system. The UV–vis spectra of $[Cu_2(dcpm)_2]X_2$ ($X = ClO_4^-$ and PF_6^-) in dichloromethane solution show intense absorption at 311 and 307 nm, respectively, with extinction coefficients greater than 10^4 dm^3 mol^{-1} cm^{-1} (Fig. 12). As the mononuclear $[Cu(PCy_3)_2]ClO_4$ complex does not exhibit any absorption at wavelengths greater than 280 nm, we assign the absorption band of $[Cu_2(dcpm)_2]X_2$ ($X = ClO_4^-$ and PF_6^-) at 311 and 307 nm to a metal–metal bonded $[3\mathrm{d}\sigma^* \rightarrow 4\mathrm{p}\sigma]$ transition. This spectral assignment has been confirmed by resonance Raman spectroscopy [16b]. The binuclear $[Cu_2(dcpm)_2]X_2$ ($X = ClO_4^-$ and PF_6^-) complexes show an absorption at 315–320 nm in acetonitrile with substantially lower extinction coefficients, revealing that coordination of acetonitrile to Cu(I) disrupts the Cu–Cu interaction, and hence the $[3\mathrm{d}\sigma^* \rightarrow 4\mathrm{p}\sigma]$ transition. The $[Cu_2(dmpm)_3]^{2+}$ complex also exhibits an intense absorption band at 276 nm ($\varepsilon = 10{,}800$ dm^3 mol^{-1} cm^{-1}) in aqueous solution, which is attributed to a $^1[3\mathrm{d}\sigma^* \rightarrow 4\mathrm{p}\sigma]$ absorption [16d].

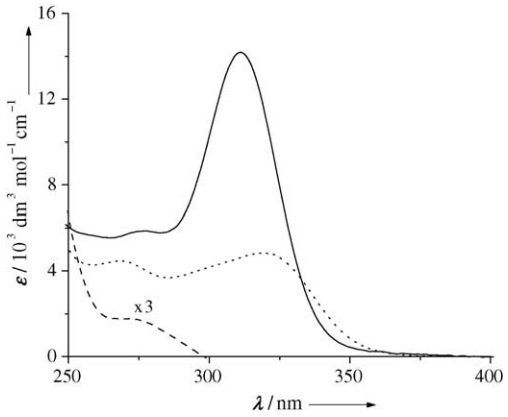

Fig. 12. Electronic absorption spectra of $[Cu_2(dcpm)_2](ClO_4)_2$ (–), $[Cu(PCy_3)_2]ClO_4$ (- - -) in dichloromethane and $[Cu_2(dcpm)_2(CH_3CN)_2](ClO_4)_2$ (···) in acetonitrile at room temperature. (Reprinted with permission from Ref. [16b]. Copyright (2000) Wiley–VCH).

The $^3[4\mathrm{p}\sigma, 3\mathrm{d}\sigma^*]$ emission from the Cu(I) system has not yet been assigned with certainty. The solid-state emission maxima of $[Cu_2(dcpm)_2]X_2$ are sensitive to the anion and coordinated solvent; $[Cu_2(dcpm)_2](ClO_4)_2$ shows phosphorescence at 475 nm, while the emission maximum of $[Cu_2(dcpm)_2(CH_3CN)_2](ClO_4)_2$ solid blue-shifts to 418 nm at room temperature. The coordinatively unsaturated Cu(I) in $[Cu_2(dcpm)_2]^{2+}$ salts can interact with solvent molecules/counterions in their vicinity and this can lead to low-energy emissions at $\lambda > 450$ nm. The weak high-energy emission of the $[Cu_2(dcpm)_2(CH_3CN)_2](ClO_4)_2$ solid at 418 nm may be assigned to the $^3[4\mathrm{p}\sigma, 3\mathrm{d}\sigma^*]$ excited state. Upon excitation at 280 nm, the mononuclear $[Cu(PCy_3)_2]X$ solids emit at 491 and 435 nm for $X = ClO_4^-$ and PF_6^-, respectively. The crystal structure of $[Cu(PCy_3)_2]PF_6$ reveals large separation between the PF_6^- ion and Cu(I), thus rendering copper–anion interactions unlikely. The red-shift in solid-state emission energy of $[Cu(PCy_3)_2]ClO_4$ can be attributed to close contact between Cu(I) and ClO_4^-, thus stabilizing the excited state through Cu–$OClO_3^-$ interaction.

4. Metal–substrate binding reactions

A simplified molecular orbital diagram illustrating the effect of substrate coordination to a two-coordinate d^{10} metal ion upon the d-orbitals is depicted in Scheme 2. Metal–substrate coordination would stabilize the [($n\mathrm{d}_{xy}$, $n\mathrm{d}_{x^2-y^2}$), $(n+1)\mathrm{p}_z$] excited state, which is generally emissive for three-coordinate d^{10} metal systems.

As early as 1980, McMillin and co-workers had suggested exciplex formation from the metal-to-ligand charge-transfer excited state of $[Cu(dmp)_2]^{+*}$ (dmp = 2,9-dimethyl-1,10-phenanthroline) with Lewis base [40]. Spectroscopic properties of the three-coordinate $[Au_2(dcpe)_3](PF_6)_2$ complex without Au(I)–Au(I) interaction were examined

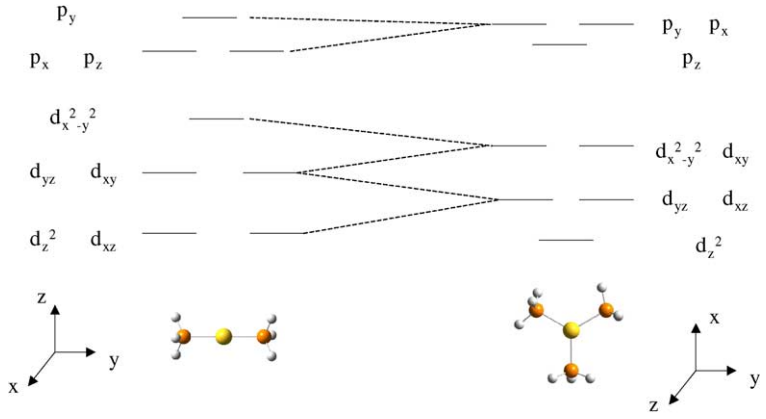

Scheme 2.

by McCleskey and Gray [15]. The $[Au_2(dcpe)_3]^{2+}$ compound is strongly emissive with $\lambda_{max} = 508$ nm ($\tau = 21.1$ μs and $\phi = 0.80$); this emission was assigned to the $^3[(5d_{x^2-y^2}, 5d_{xy})(6p_z)]$ excited state of three-coordinate Au(I). The important role of three-coordinate Au(I) in gold(I) photoluminescence was also illustrated by Che and co-workers [41]. The two-coordinate $[Au(P^{\cap}P)]^+$ ($P^{\cap}P$ = 1,8-bis(diphenylphosphino)-3,6-dioxaoctane) complex is non-emissive in solution, however, upon addition of one equivalent of PPh_3, an intense emission at $\lambda_{max} = 500$ nm was 'switched on' (Scheme 3, Fig. 13), and ground-state complexation of $[Au(P^{\cap}P)]^+$ by PPh_3 to give the emissive $[Au(P^{\cap}P)PPh_3]^+$ species was proposed.

With non-coordinating or weakly coordinating solvent molecules/anions, it is difficult to observe substrate binding

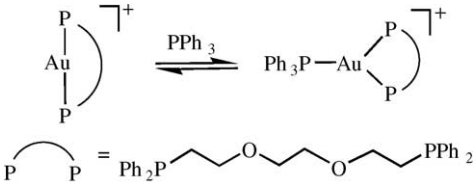

Scheme 3. Equilibrium between $[Au(P^{\cap}P)]^+$ and PPh_3 in solution.

reactions involving two-coordinate Au(I) in the ground state by spectroscopic means. However, as described in the following section, substrate binding reactions of Au(I) in the excited state, even with non- or weakly-coordinating anion, are facile and can be studied by time-resolved absorption and emission spectroscopy.

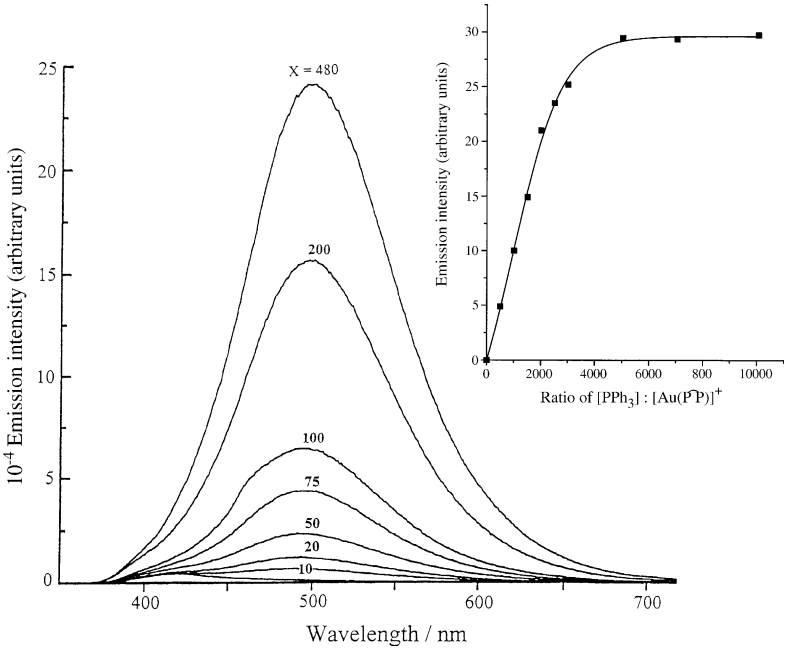

Fig. 13. Room temperature emission spectra of $[Au(P^{\cap}P)](ClO_4)$ in the presence of PPh_3 in degassed acetonitrile solution. Molar ratio of PPh_3:$[Au(P^{\cap}P)]^+$ = X:1. Inset: a plot of the emission intensity of $[Au(P^{\cap}P)(PPh_3)]^+$ vs. X:1 (concentration of $[Au(P^{\cap}P)](ClO_4) = 10^{-5}$ mol dm^{-3}) (Reprinted with permission from Ref. [41]. Copyright (1998) Royal Society of Chemistry).

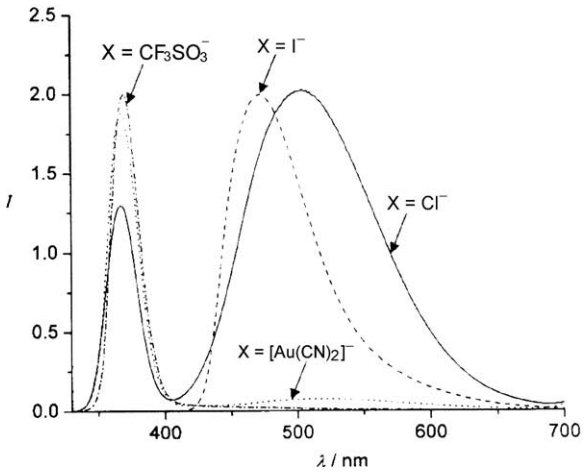

Fig. 14. Room-temperature solid-state emission spectra of $[Au_2(dcpm)_2]X_2$ ($X = CF_3SO_3^-$, $Au(CN)_2^-$, Cl^-, and I^-) with excitation at $\lambda = 280$ nm. *I*, intensity (Reprinted with permission from Ref. [16c]. Copyright (2001) Wiley–VCH).

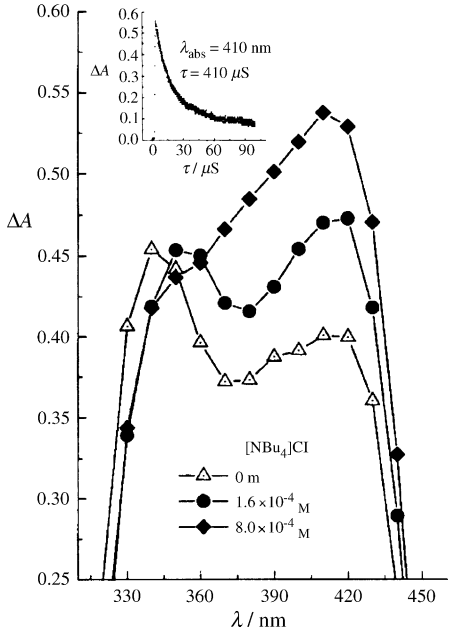

Fig. 15. Room-temperature transient difference-absorption spectra of $[Au_2(dcpm)_2]Cl_2$ (7.5×10^{-5} mol dm^{-3}) in various $[NBu_4Cl]$ concentrations monitored after 1.5 μs pulsed excitation at $\lambda = 266$ nm in degassed acetonitrile solution. Inset: decay traces of transient difference-absorption spectra of $[Au_2(dcpm)_2]Cl_2$ (7.5×10^{-5} mol dm^{-3}) in $[NBu_4]Cl$ (8.0×10^{-4} mol dm^{-3}) monitored at $\lambda = 410$ nm. (Reprinted with permission from Ref. [16c]. Copyright (2001) Wiley–VCH).

In previous sections, we reported that the $[Au_2(dcpm)_2]X_2$ (where X is the non-coordinating ClO_4^-, PF_6^-, or $Au(CN)_2^-$ anion) solids show high-energy $^3[6p\sigma, 5d\sigma^*]$ emission at 368 nm. These $Au_2(dcpm)_2]X_2$ solids, however, also display weak visible emissions at $\lambda = 564$, 505, and 515 nm for $X = ClO_4^-$, PF_6^-, and $Au(CN)_2^-$, respectively. These lower-energy (500–570 nm) emissions are assigned to triplet-excited states since their lifetimes are in the microsecond regime.

For the $[Au_2(dcpm)_2]I_2$ and $[Au_2(dcpm)_2](SCN)_2$ solids, the lower-energy visible emission becomes more dominant with λ_{max} at 465 and 473 nm, respectively, while their $^3[6p\sigma, 5d\sigma^*]$ emission becomes diminished. We found that an increase in the Au(I)–anion interaction enhances the intensity of the visible emission from the $[Au_2(dcpm)_2]X_2$ solids [16c]. The closer the cation···anion contacts, the stronger would be the effect of the neighboring anion on the $^3[6p\sigma, 5d\sigma^*]$ excited state of $[Au_2(dcpm)_2]^{2+}$, and hence exciplex-adduct formation is more likely (Fig. 14). Complex $[Au_2(dcpm)_2]Cl_2$ displays both high- and low-energy emissions with λ_{max} at 366 and 505 nm, respectively. The crystal structure of $[Au_2(dcpm)_2]Cl_2$ reveals a Au···Cl contact of 2.7755(9) Å, which is shorter than those of Au···I (2.9960(7) Å) and Au···SCN (3.011(3) Å) in $[Au_2(dcpm)_2]X_2$ ($X = I^-$ and SCN^-). Interestingly, the energy of the low-energy solid-state emission follows the order: $[Au_2(dcpm)_2]Cl_2$ (505 nm) < $[Au_2(dcpm)_2]I_2$ (473 nm) < $[Au_2(dcpm)_2](SCN)_2$ (465 nm). The low-energy visible emission is hence attributed to exciplex formation between the $[Au_2(dcpm)_2]^{2+}$ core and X^-.

At room temperature, $[Au_2(dcpm)_2]X_2$ ($X = ClO_4^-$, PF_6^-, $CF_3SO_3^-$, $Au(CN)_2^-$, Cl^-, SCN^-, and I^-) complexes show emission in acetonitrile with λ_{max} ranging from 490 to 530 nm, but the $^3[6p\sigma, 5d\sigma^*]$ emission at 368 nm is extremely weak. For $[Au_2(dcpm)_2]I_2$, complexation of $[Au_2(dcpm)_2]^{2+}$ by iodide in the ground state is evident from absorption spectroscopy. We assign the visible emission of acetonitrile solutions of $[Au_2(dcpm)_2]X_2$ to originate from exciplex formation between the $[Au_2(dcpm)_2]^{2+*}$ core and CH_3CN molecules. This assignment is also supported by calculations [38]. Using $[Au_2(H_2PCH_2PH_2)_2]^{2+}\cdot(MeCN)_2$ as a model, the mean calculated Au–N distances is 2.583 Å, indicating that the MeCN molecules only weakly coordinate to Au(I) in the ground state. However, in the ^3A_u excited state of $[Au_2(H_2PCH_2PH_2)_2]^{2+}\cdot(MeCN)_2$, the Au–N distance was calculated to be 2.377 Å, reflecting enhanced interaction between Au(I) and the CH_3CN molecules. The $[^3A_u \rightarrow {}^3A_g]$ transition of $[Au_2(H_2PCH_2PH_2)_2]^{2+}\cdot(MeCN)_2$ was calculated to occur at 557 nm, which approaches the 575-nm emission for $[Au_2(dppm)_2](ClO_4)_2$ and the 510-nm emission for $[Au_2(dcpe)_2](ClO_4)_2$ in acetonitrile solution at room temperature. The calculated Au–Au distance of 2.719 Å in the ^3A_u excited state of $[Au_2(H_2PCH_2PH_2)_2]^{2+}\cdot(MeCN)_2$ reveals formation of Au–Au single bond and the Au–Au interaction is further enhanced through coordination of MeCN to the gold atoms.

The triplet-state difference absorption spectrum of $[Au_2(dcpm)_2]Cl_2$ in acetonitrile was measured at different concentrations of $[NBu_4]Cl$ (Fig. 15). The 350-nm absorption maximum, which comes from the triplet excited state of $[Au_2(dcpm)_2]^{2+}$, is shifted to 410 nm in the presence of $[NBu_4]Cl$, thus reflecting complexation of $[Au_2(dcpm)_2]^{2+*}$ with Cl^- to give $[Au_2(dcpm)_2Cl]^{+*}$.

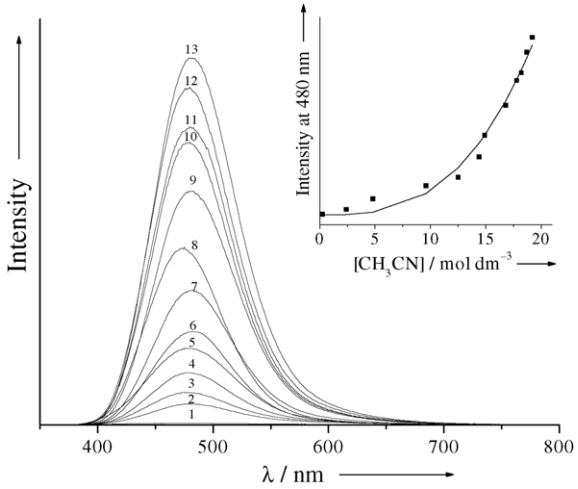

Fig. 16. Emission spectral changes of $[Cu_2(dcpm)_2](PF_6)_2$ (2.4×10^{-4} mol dm^{-3}) in CH_2Cl_2 upon addition of CH_3CN ($\lambda_{ex} = 310$ nm) at 298 K. Concentration of CH_3CN: (1) 0.05, (2) 0.24, (3) 2.4, (4) 4.8, (5) 9.6, (6) 12.5, (7) 14.4, (8) 14.9, (9) 16.6, (10) 17.8, (11) 18.2, (12) 18.7, (13) 19.2 mol dm^{-3}. Inset: Emission intensity at 480 nm vs. $[CH_3CN]$ and theoretical fitting curve. (Reprinted with permission from Ref. [16d]. Copyright (2003) Wiley–VCH).

$$\underset{350\,nm}{[Au_2(dcpm)_2^{2+}]^*} + Cl^- \rightleftharpoons \underset{410\,nm}{[Au_2(dcpm)_2Cl^+]^*}$$

Complexes $[Cu_2(dcpm)_2]X_2$ and $[Cu_2(dcpm)_2(CH_3CN)_2]X_2$ ($X = ClO_4^-$ and PF_6^-) emit very weakly in CH_2Cl_2 ($\phi < 10^{-4}$), but emission at ~480 nm is 'switched on' upon addition of CH_3CN [16d]. Fig. 16 shows the increase in emission intensity upon addition of CH_3CN to a solution of $[Cu_2(dcpm)_2](PF_6)_2$ in CH_2Cl_2. A non-linear plot of emission intensity at 480 nm versus CH_3CN concentration was observed (inset of Fig. 16); the greatest intensity at 480 nm was found in pure CH_3CN. The emission data match the fitting curve for $n = 3$ and we proposed that the number of CH_3CN molecules (n) coordinated with the $[Cu_2(dcpm)_2]^{2+}$ is not less than three. It appears that the intense 480 nm emission comes from coordination of CH_3CN molecules to Cu(I), leading to the formation of a strongly emissive $^3[(d_{x^2-y^2}, d_{xy})(p_z)]$ excited state from a three- or four-coordinate Cu(I) site.

$$Cu_2(dcpm)_2]^{2+} + nCH_3CN \overset{K}{\rightleftharpoons} [Cu_2(dcpm)_2(CH_3CN)_n]^{2+}$$

($n \geq 3$)

5. Photochemistry

The $[Au_2(P\cap P)_2]^{2+}$ and $[Cu_2(P\cap P)_2]^{2+}$ systems are powerful photo-reductants, and light-induced electron transfer reactions with pyridinium acceptors have been demonstrated. Quenching studies with a series of pyridinium acceptors established the E° values of both $[Au_2(dppm)_2]^{3+/2+*}$ and $[Au_2(dmpm)_3]^{3+/2+*}$ to be $-1.6(1)$ V. However, in acetonitrile, steady-state photolysis revealed no net chemical reaction. The triplet excited states of the $[Cu_2(dcpm)_2]^{2+}$ and $[Cu_2(dmpm)_3]^{2+}$ (dmpm = bis(dimethylphosphino)methane) complexes are also powerful reductants [16d]. For example, the emission of $[Cu_2(dmpm)_3](ClO_4)_2$ was quenched by pyridinium acceptors through an electron transfer mechanism. Fig. 17 shows the transient absorption difference spectrum of a CH_3CN solution of $[Cu_2(dmpm)_3]^{2+}$ and MV^{2+} recorded 1 μs after laser flashing at 355 nm.

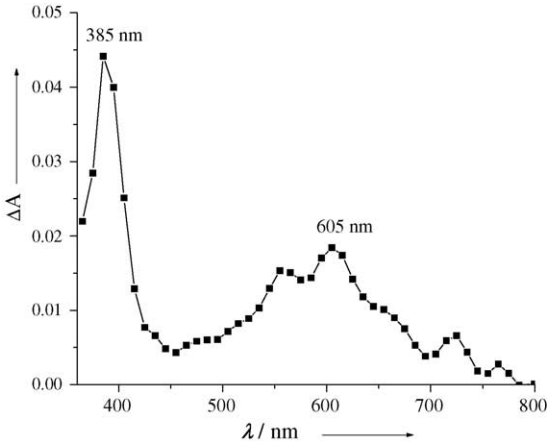

Fig. 17. Transient absorption difference spectrum recorded 1 μs after laser flashing for a solution of $[Cu_2(dmpm)_3]^{2+}$ (2.21×10^{-4} mol dm^{-3}) and MV^{2+} (1.12×10^{-2} mol dm^{-3}) in CH_3CN. (Reprinted with permission from Ref. [16d]. Copyright (2003) Wiley–VCH).

The two absorption maxima at 385 and 605 nm are due to $MV^{\bullet+}$, and the decay of absorbance at these two wavelengths followed second-order kinetics (rate constant = 6.9×10^7 dm^3 mol^{-1} s^{-1}). The proposed photochemical reaction is depicted in Scheme 4.

Other pyridinium acceptors also quenched the 509-nm emission of $[Cu_2(dmpm)_3]^{2+*}$, and the quenching rate constants were determined by Stern–Volmer kinetics experiments. Upon fitting the rate constants using the Rehm–Weller equation, the excited-state redox potential ($E^\circ[Cu_2(dmpm)_3{}^{3+/2+*}]$) was determined to be -1.55 V versus SSCE and the reorganization energy (λ) is 0.76 eV [16d].

The emission of $[Cu_2(dcpm)_2]^{2+}$ salts were also quenched by pyridinium acceptors, but net steady-state photochemistry was not observed in acetonitrile. However, in the presence of ethanol or methanol, a facile net photoredox reaction was observed upon laser-flash photolysis of a solution of $[Cu_2(dcpm)_2](PF_6)_2$ and MV^{2+} (Fig. 18).

The absorbance at 607 nm attributed to $MV^{\bullet+}$ did not decay but reached a maximum after irradiation for 35 min, while the absorbance of MV^{2+} at $\lambda_{max} = 260$ nm decreased

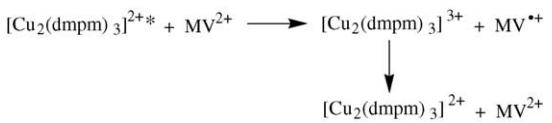

Scheme 4.

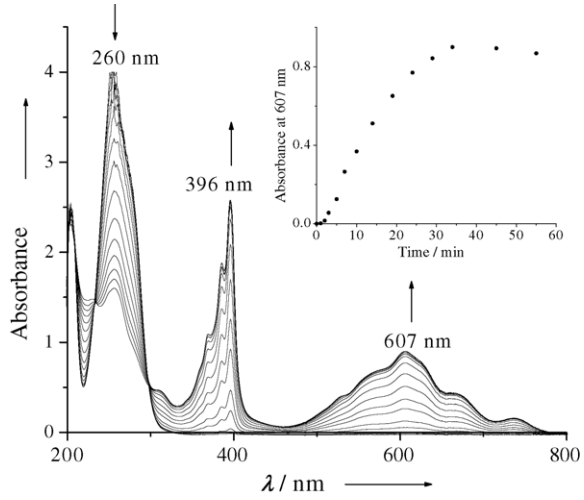

Fig. 18. UV–vis spectral changes of $[Cu_2(dcpm)_2](PF_6)_2$ (9.71×10^{-6} mol dm^{-3}) and MV^{2+} (2.04×10^{-4} mol dm^{-3}) in ethanol as a function of irradiation time. Inset: absorbance at 607 nm as a function of irradiation time. (Reprinted with permission from Ref. [16d]. Copyright (2003) Wiley–VCH).

with irradiation. This suggests that the photochemically generated $[Cu^ICu^{II}(dcpm)_2]^{3+}$ species reacted with alcohol to regenerate the $[Cu_2(dcpm)_2]^{2+}$ precursor. A two-coordinate Cu(I) site is essential since the $[Cu_2(dmpm)_3]^{2+}$ complex did not undergo a similar photochemical reaction with MV^{2+} in acetonitrile or in the presence of ethanol or methanol. It appears that two-coordinate Cu(II) generated in situ by photochemical means is a highly reactive species and could rapidly react with alcohol, thus prohibiting back electron transfer reactions. The $[Cu_2(dppm)_2(CH_3CN)_4]^{2+}$ complex was reported to catalyze light-induced carbon–carbon coupling reactions of alkyl halides [7] and the photochemical reactions could involve binding of alkyl halide to Cu(I) in the excited state.

6. Concluding remarks

This review provides an overview of the structural and spectroscopic investigations into the photoluminescent di- and tri-nuclear coinage metal complexes $[M_2(P^{\cap}P)_2]X_2$ and $[M_3(P^{\cap}P^{\cap}P)_2]X_3$. The intramolecular M(I)−M(I) separations in these d^{10} metal complexes fall in the range of 2.9–3.1 Å for Ag(I) and Au(I), and 2.6–2.8 Å for Cu(I), which are shorter than the sum of van der Waals radii of M(I), and are therefore prone to weak closed-shell d^{10}–d^{10} interactions. Interestingly, close metal-anion contacts are usually encountered in the crystal lattices of the two-coordinate d^{10} metal solids, and such interactions are apparently more pronounced in Cu(I) than Au(I).

The existence of M(I)–M(I) interaction in the [ndσ*, (n + 1)pσ] excited states could be inferred by the occurrence of an intense red-shifted absorption attributed to the [ndσ$^* \rightarrow$ (n + 1)pσ] transition, the assignment of which was supported by resonance Raman spectroscopy. For the di- and tri-nuclear Au(I) complexes, the ^{3}[(n + 1)pσ, ndσ*] emission in the UV region has been recorded.

The metal-ligand coordination in both ground and excited states would stabilize the ^{3}[(nd$_{x^2-y^2}$, nd$_{xy}$), (n + 1)p$_z$] state of a three-coordinate M(I) site, which is generally emissive and could be lower in energy than the ^{3}[(n + 1)pσ, ndσ*] emission. For example, the excited two-coordinate $^*Cu(CN)_2^-$, formed upon UV irradiation in aqueous solution, was reported to coordinate with halide ion to give a long-lived, highly luminescent exciplex [42]. Interestingly, such emissions are usually observed at $\lambda \geq 400$ nm, and hence lower in energy than the ^{3}[(n + 1)pσ, ndσ*] excited states of the di-nuclear $[Cu_2(P^{\cap}P)_2]^{2+}$ complexes.

The photochemistry of two-coordinate d^{10} metal complexes is an area of potential interest in the context of developing new photocatalysts. Studies in this area remain sparse. The observation that net steady-state photochemical reduction of MV^{2+} to $MV^{\bullet+}$ can be achieved with $[Cu_2(dcpm)_2]^{2+}$ in the presence of ethanol or methanol suggests that highly reactive two-coordinate d^9 Cu(II) species generated photochemically could have a rich oxidation chemistry.

Acknowledgements

We are grateful for financial support from the University Development Fund of The University of Hong Kong, the Hong Kong University Foundation, and the Research Grants Council of the Hong Kong SAR, China [HKU 7039/03P].

References

[1] (a) A.P. Zipp, Coord. Chem. Rev. 84 (1988) 47;
(b) D.M. Roundhill, H.B. Gray, C.-M. Che, Acc. Chem. Res. 22 (1989) 55, and references therein.
[2] R.F. Ziolo, S. Lipton, Z. Dori, J. Chem. Soc. Chem. Commun. (1970) 1124.
[3] A. Vogler, H. Kunkely, J. Am. Chem. Soc. 108 (1986) 7211.
[4] C. King, J.-C. Wang, M.N.I. Khan, J.P. Fackler Jr., Inorg. Chem. 28 (1989) 2145.
[5] C.-M. Che, H.-L. Kwong, V.W.-W. Yam, K.-C. Cho, J. Chem. Soc. Chem. Commun. (1989) 885.
[6] C.-M. Che, H.-L. Kwong, C.-K. Poon, V.W.-W. Yam, J. Chem. Soc. Dalton Trans. (1990) 3215.
[7] D. Li, C.-M. Che, H.-L. Kwong, V.W.-W. Yam, J. Chem. Soc. Dalton Trans. (1992) 3325.
[8] (a) M.J. Irwin, J.J. Vittal, R.J. Puddephatt, Organometallics 16 (1997) 3541;
(b) V.W.-W. Yam, K.K.-W. Lo, Chem. Soc. Rev. 28 (1999) 323;
(c) M.A. Rawashdeh-Omary, M.A. Omary, J.P. Fackler Jr., R. Galassi, B.R. Pietroni, A. Burini, J. Am. Chem. Soc. 123 (2001) 9689;
(d) R.L. White-Morris, M.M. Olmstead, A.L. Balch, J. Am. Chem. Soc. 125 (2003) 1033;
(e) E.J. Fernandez, J.M. Lopez-de-Luzuriaga, M. Monge, M.E. Olmos, J. Perez, A. Laguna, A.A. Mohamed, J.P. Fackler Jr., J. Am. Chem. Soc. 125 (2003) 2022;
(f) Y.-A. Lee, R. Eisenberg, J. Am. Chem. Soc. 125 (2003) 7778.

[9] (a) M. Jansen, Angew. Chem. Int. Ed. Engl. 26 (1987) 1098;
(b) M.J. Irwin, G. Jia, N.C. Payne, R.J. Puddephatt, Organometallics 15 (1996) 51;
(c) P. Pyykkö, Chem. Rev. 97 (1997) 597;
(d) P. Pyykkö, F. Mendizabal, Inorg. Chem. 37 (1998) 3018;
(e) R.J. Puddephatt, Coord. Chem. Rev. 216–217 (2001) 313;
(f) W.J. Hunks, M.C. Jennings, R.J. Puddephatt, Inorg. Chem. 41 (2002) 4590.
[10] (a) H. Schmidbaur, Gold Bull. 23 (1990) 11;
(b) H. Schmidbaur, Chem. Soc. Rev. 24 (1995) 391;
(c) C. Hollatz, A. Schier, H. Schmidbaur, J. Am. Chem. Soc. 119 (1997) 8115.
[11] (a) S.-J. Shieh, X. Hong, S.-M. Peng, C.-M. Che, J. Chem. Soc. Dalton Trans. (1994) 3067;
(b) B.-C. Tzeng, K.-K. Cheung, C.-M. Che, Chem. Commun. (1996) 1681.
[12] V.W.-W. Yam, K.K.-W. Lo, W.K.-M. Fung, C.-R. Wang, Coord. Chem. Rev. 171 (1998) 17.
[13] (a) J.C. Vickery, M.M. Olmstead, E.Y. Fung, A.L. Balch, Angew. Chem. Int. Ed. Engl. 36 (1997) 1179;
(b) M.A. Mansour, W.B. Connick, R.J. Lachicotte, H.J. Gysling, R. Eisenberg, J. Am. Chem. Soc. 120 (1998) 1329;
(c) E. Cariati, J. Bourassa, P.C. Ford, Chem. Commun. (1998) 1623.
[14] V.J. Catalano, H.M. Kar, J. Garnas, Angew. Chem. Int. Ed. 38 (1999) 1979.
[15] T.M. McCleskey, H.B. Gray, Inorg. Chem. 31 (1992) 1733.
[16] (a) W.-F. Fu, K.-C. Chan, V.M. Miskowski, C.-M. Che, Angew. Chem. Int. Ed. 38 (1999) 2783;
(b) C.-M. Che, Z. Mao, V.M. Miskowski, M.-C. Tse, C.-K. Chan, K.-K. Cheung, D.L. Phillips, K.-H. Leung, Angew. Chem. Int. Ed. 39 (2000) 4084;
(c) W.-F. Fu, K.-C. Chan, K.-K. Cheung, C.-M. Che, Chem. Eur. J. 7 (2001) 4656;
(d) Z. Mao, H.-Y. Chao, Z. Hui, C.-M. Che, W.-F. Fu, K.-K. Cheung, N. Zhu, Chem. Eur. J. 9 (2003) 2885.
[17] A. Bondi, J. Phys. Chem. 68 (1964) 441.
[18] J. Díez, M.P. Gamasa, J. Gimeno, A. Tiripicchio, M.T. Camellini, J. Chem. Soc. Dalton Trans. (1987) 1275.
[19] D. Li, C.-M. Che, W.-T. Wong, S.-J. Shieh, S.-M. Peng, J. Chem. Soc. Dalton Trans. (1993) 653.
[20] D. Li, H.-K. Yip, C.-M. Che, Z.-Y. Zhou, T.C.W. Mak, S.-T. Liu, J. Chem. Soc. Dalton Trans. (1992) 2445.
[21] C.-M. Che, M.-C. Tse, M.C.W. Chan, K.-K. Cheung, D.L. Phillips, K.-H. Leung, J. Am. Chem. Soc. 122 (2000) 2464.
[22] (a) D.M. Ho, R. Bau, Inorg. Chem. 22 (1983) 4073;
(b) R.I. Papasergio, C.L. Raston, A.H. White, J. Chem. Soc. Chem. Commun. (1984) 612;
(c) T. Tsuda, S. Ohba, M. Takahashi, M. Ito, Acta Crystallogr. C45 (1989) 887;
(d) X.-M. Chen, T.C.W. Mak, J. Chem. Soc. Dalton Trans. (1991) 1219;
(e) F. Robinson, M.J. Zaworotko, J. Chem. Soc. Chem. Commun. (1995) 2413;
(f) T. Ren, C. Lin, P. Amalberti, D. Macikenas, J.D. Protasiewicz, J.C. Baum, T.L. Gibson, Inorg. Chem. Commun. 1 (1998) 23;
(g) R. Villanneau, A. Proust, F. Robert, P. Gouzerh, Chem. Commun. (1998) 1491;
(h) T. Chivers, M. Parvez, G. Schatte, Angew. Chem. Int. Ed. 38 (1999) 2217;
(i) J. Zank, A. Schier, H. Schmidbaur, J. Chem. Soc. Dalton Trans. (1999) 415.
[23] H.H. Karsch, U.Z. Schubert, Naturforsh 37B (1982) 186.
[24] C.-M. Che, H.-K. Yip, D. Li, S.-M. Peng, G.-H. Lee, Y.-M. Wang, S.-T. Liu, J. Chem. Soc. Chem. Commun. (1991) 1615.
[25] A.A.M. Aly, D. Neugebauer, O. Orama, U. Schubert, H. Schmidbaur, Angew. Chem. Int. Ed. Engl. 17 (1978) 125.
[26] H. Schmidbaur, A. Wohlleben, U. Schubert, A. Frank, G. Huttner, Chem. Ber. 110 (1977) 2751.
[27] J.-C. Wang, M.N.I. Khan, J.P. Fackler Jr., Acta Crystallogr. C45 (1989) 1482.
[28] L.C. Porter, M.N.I. Khan, C. King, J.P. Fackler Jr., Acta Crystallogr. C45 (1989) 947.
[29] M.N.I. Khan, C. King, D.D. Heinrich, J.P. Fackler Jr., L.C. Porter, Inorg. Chem. 28 (1989) 2150.
[30] H.-R.C. Jaw, M.M. Savas, R.D. Rogers, W.R. Mason, Inorg. Chem. 28 (1989) 1028.
[31] W.P. Schaefer, R.E. Marsh, T.M. McCleskey, H.B. Gray, Acta Crystallogr. C47 (1991) 2553.
[32] T.M. McCleskey, L.M. Henling, K.A. Flanagan, H.B. Gray, Acta Crystallogr. C49 (1993) 1467.
[33] V.W.-W. Yam, T.-F. Lai, C.-M. Che, J. Chem. Soc. Dalton Trans. (1990) 3747.
[34] D. Li, C.-M. Che, S.-M. Peng, S.-T. Liu, Z.-Y. Zhou, T.C.W. Mak, J. Chem. Soc. Dalton Trans. (1993) 189.
[35] K.H. Leung, D.L. Phillips, M.-C. Tse, C.-M. Che, V.M. Miskowski, J. Am. Chem. Soc. 121 (1999) 4799.
[36] G.P. Fenske Jr., W.R. Mason, Inorg. Chem. 13 (1974) 1783.
[37] W. Ludwig, W. Meyer, Helv. Chim. Acta 65 (1982) 934.
[38] H.-X. Zhang, C.-M. Che, Chem. Eur. J. 7 (2001) 4887.
[39] C.-M. Che, G.S.-M. Tong, unpublished results.
[40] (a) M.W. Blaskie, D.R. McMillin, Inorg. Chem. 19 (1980) 3519;
(b) E.M. Stacy, D.R. McMillin, Inorg. Chem. 29 (1990) 393.
[41] W.-H. Chan, T.C.W. Mak, C.-M. Che, J. Chem. Soc. Dalton Trans. (1998) 2275.
[42] (a) A. Horváth, K.L. Stevenson, Inorg. Chim. Acta 186 (1991) 61;
(b) A. Horváth, K.L. Stevenson, Inorg. Chem. 32 (1993) 2225;
(c) A. Horváth, C.E. Wood, K.L. Stevenson, J. Phys. Chem. 98 (1994) 6490;
(d) A. Horváth, C.E. Wood, K.L. Stevenson, Inorg. Chem. 33 (1994) 5351.